

1 **A review of recent updates of sea-level projections at global and regional scales**

2

3 A. B. A. Slangen^{1,2*}, F. Adloff³, S. Jevrejeva⁴, P. W. Leclercq⁵, B. Marzeion⁶, Y.
4 Wada^{7,8,9,10}, R. Winkelmann¹¹

5

6 ¹CSIRO Oceans and Atmosphere, Hobart, Tasmania, Australia

7 ²Institute for Marine and Atmospheric research Utrecht, Utrecht University, Utrecht,
8 The Netherlands

9 ³CNRM-GAME, Météo-France, CNRS, Toulouse, France

10 ⁴National Oceanographic Centre, Liverpool, UK

11 ⁵Department of Geosciences, University of Oslo, Oslo, Norway

12 ⁶Institute of Geography, University of Bremen, Bremen, Germany

13 ⁷NASA Goddard Institute for Space Studies, Columbia University, New York, USA

14 ⁸Center for Climate Systems Research, Columbia University, New York, USA

15 ⁹Department of Physical Geography, Utrecht University, Utrecht, The Netherlands

16 ¹⁰International Insitute for Applied Systems Analysis, Laxenburg, Austria

17 ¹¹Potsdam Institute for Climate Impact Research, University of Potsdam, Potsdam,
18 Germany

19 *Corresponding author: aimee.slangen@gmail.com

20

21

22 **Abstract**

23

24 Sea-level change (SLC) is a much-studied topic in the area of climate research,
25 integrating a range of climate science disciplines, and is expected to impact coastal
26 communities around the world. As a result, this field is rapidly moving and the
27 knowledge and understanding of processes contributing to SLC is increasing. Here,
28 we discuss noteworthy recent developments in the projection of SLC contributions
29 and in the global mean and regional sea-level projections. For the Greenland ice
30 sheet contribution to SLC, earlier estimates have been confirmed in recent research,
31 but part of the source of this contribution has shifted from dynamics to surface
32 melting. New insights into dynamic discharge processes and the onset of marine ice-
33 sheet instability bring the estimated Antarctic contribution to SLC at 0.3-0.4 m by
34 2100. The contribution from both ice sheets is projected to increase in the coming
35 centuries to millennia. Recent updates of the global glacier outline database and
36 new global glacier models have led to slightly lower projections for the glacier
37 contribution to SLC (in the order of 0.12-0.13 m by 2100), but still project the glaciers
38 to be an important contribution. For global mean sea-level projections, the focus has
39 shifted to better estimating the uncertainty distributions of the projection time
40 series, which may not necessarily follow a normal distribution. Instead, recent
41 studies use skewed distributions with longer tails to higher uncertainties. Regional
42 projections have been used to study regional uncertainty distributions, and regional
43 projections are increasingly being applied to specific regions, countries and coastal
44 areas.

45

46 **1. Introduction**

47 As one of the most well-known consequences of climate change, sea-level change
48 (SLC) is relevant to coastal communities and stakeholders around the world. A large
49 number of the world's population (~10% [*McGranahan et al.*, 2007]) lives and works
50 near the coast and depends on the ocean as their primary source of food and
51 livelihood. An increase in mean sea level can increase the impacts of storm surges
52 and the risk of flooding events in coastal zones [*Wong et al.*, 2013]. To make well-
53 informed decisions about protective or adaptive measures, it is crucial that decision
54 makers are provided with the best possible projections of SLC. Projecting future SLC
55 and understanding the physical processes that contribute to SLC is therefore an
56 important and rapidly evolving research topic.

57

58 SLC is a result of changes in many different parts of the climate system and can
59 therefore be seen as an integrative measure of climate change. Over 90% of the
60 energy that is stored in the climate system ends up in the ocean [*Rhein et al.*, 2013],
61 causing thermal expansion and sea-level rise. In addition, ice sheets and glaciers lose
62 mass due to increasing temperatures (both atmospheric and in the ocean [*Vaughan*
63 *et al.*, 2013]) and reservoirs of water on land change due to human intervention
64 [*Church et al.*, 2013], which not only changes the amount of water in the oceans, but
65 also the Earth's gravitational field. The solid Earth also responds to the redistribution
66 of mass on the Earth surface both for present-day and for distant past (Last Glacial
67 Maximum, ~20,000 years ago) mass variations, changing the height of the ocean
68 floor. In the past century, global mean sea level has already increased by 19 ± 2 cm
69 (1901-2010, [*Church et al.*, 2013]), a rise that is expected to continue and accelerate
70 in the coming centuries.

71

72 The Intergovernmental Panel on Climate Change Fifth Assessment Report (IPCC AR5)
73 chapter on Sea Level Rise [*Church et al.*, 2013] presented a comprehensive
74 assessment of papers up to the IPCC working group 1 cut-off date of March 2013. In
75 the chapter, important strides were made compared to the IPCC Fourth Assessment
76 report (AR4) by progress in closing the 20th century sea-level budget, the addition of
77 an assessment of the ice-sheet dynamical contribution to SLC and by making regional

78 sea-level projections for the 21st century. However, a lot of research has been
79 completed since IPCC AR5 and the lead authors of the chapter on SLC have recently
80 published an update of their work [*Clark et al.*, 2015]. Here, we also focus on work
81 that has been published since AR5 and aim to complement the review by *Clark et al.*
82 [2015] by including more recent publications for the different contributions where
83 available and by presenting overviews of research on the terrestrial water storage
84 (TWS) contribution and the Mediterranean region, which were not discussed in *Clark*
85 *et al.* [2015]. The case of the Mediterranean is chosen because it is an area that is
86 vulnerable to SLC due to the high population densities around the basin, and a lot of
87 sea-level research is done specifically for this region.

88

89 First we present an overview of recent work on contributions to SLC due to mass
90 changes of glaciers and ice sheets (Section 2) and TWS changes (Section 3). Then, we
91 will discuss global mean sea-level projections and new ways to treat the
92 uncertainties thereof (Section 4). Recent advances in and uses of regional sea-level
93 projections are presented in Section 5. Thermal expansion and dynamical ocean
94 fields are not discussed in a separate section but are included in Sections 4 and 5, as
95 the most up-to-date projections are based on climate model output which has not
96 changed since IPCC AR5. Finally, Section 6 presents research on sea-level projections
97 in the Mediterranean region.

98

99 **2. Land ice mass change projections**

100

101 **2.1 Ice Sheet projections**

102 The ice sheets on Greenland and Antarctica are by far the largest potential source of
103 future SLC, storing approximately 65 m sea-level equivalent (SLE, *Vaughan et al.*
104 [2013], *Clark et al.* [2015]). Both ice sheets have increasingly lost mass in the past
105 decades [*Rignot et al.*, 2011] and are expected to dominate the sea-level budget on
106 the long term [*Church et al.*, 2013].

107

108 **Greenland** Mass loss from Greenland is controlled by changes in surface mass
109 balance (SMB) and dynamic discharge, including the effects of basal lubrication and
110 ocean warming. IPCC AR5 [*Church et al.*, 2013] estimated that Greenland would
111 contribute between 0.04 - 0.10 m for RCP2.6 (Representative Concentration
112 Pathway, *Moss et al.*, [2010]) scenario and 0.07 - 0.21 m for RCP8.5 by the end of this
113 century. For the lower emission scenarios, surface melting and dynamic discharge
114 were expected to contribute equally to the overall mass loss. For emission scenario
115 RCP8.5, the mass balance was projected to be dominated by increased melting at
116 the surface.

117

118 If a certain threshold is passed, the feedback between the lowering surface elevation
119 and increasing surface melting can lead to additional ice loss and eventually even the
120 complete loss of the Greenland Ice Sheet [*Ridley et al.*, 2010; *Robinson et al.*, 2012].
121 *Edwards et al.* [2014] found that this positive feedback might be less significant for
122 this century than previously expected. They estimate the surface elevation feedback
123 to account for at most an additional 6.9 % ice loss from Greenland as opposed to the
124 15 % estimated in AR5. Other recent studies confirm the conclusion from AR5 that
125 basal lubrication will likely not have a significant effect on Greenland mass loss
126 within this century [*Shannon et al.*, 2013].

127

128 Based on a higher-order ice-sheet model driven by temperature changes from
129 Atmosphere-Ocean Global Climate Model (AOGCM) results, *Fürst et al.* [2015]
130 project a Greenland contribution of 0.01–0.17 m to SLC within the 21st century in

131 response to both atmospheric and oceanic warming. In contrast to previous studies,
132 they conclude that future ice loss will be dominated by surface melting rather than
133 dynamic discharge because the marine ice margin will retreat over time, reducing
134 the contact area between ice and ocean water and thus limiting dynamic discharge.
135 For the two lower emission scenarios, RCP2.6 and RCP4.5, simulations yield a
136 contribution to SLC between 0.03 and 0.32 m by 2300 (Figure 1). These new
137 projections thus fall within the AR5 likely ranges but with a higher contribution from
138 surface melting as opposed to dynamic discharge [Clark *et al.*, 2015].

139

140 **Antarctica** The mass balance of the Antarctic Ice Sheet is determined by changes in
141 the SMB as well as changes of the ice flux across the grounding line resulting from
142 enhanced basal sliding, calving or sub-shelf melting. Since surface melting will
143 remain negligible within the 21st century [Vizcaino *et al.*, 2010; Huybrechts *et al.*,
144 2011], the SMB is predominantly determined by snow accumulation. Evidence from
145 paleo data and projections from global and regional climate models show that
146 snowfall in Antarctica is very likely to increase with future atmospheric warming
147 [Frieler *et al.*, 2015]. The resulting mass gain might however be compensated or even
148 overcompensated by dynamic effects [Winkelmann *et al.*, 2012].

149

150 In AR5, the overall contribution of Antarctica to SLC was estimated to range from -
151 0.04 to 0.16 m for RCP2.6 and -0.08 to 0.14 m for RCP8.5 by 2100 compared to 1986-
152 2005 [Church *et al.*, 2013]. The SLC arising from rapid dynamics was projected to be -
153 0.02 to 0.19 m, deduced from a combination of model results, expert judgement and
154 statistical extrapolation of current trends. Due to insufficient understanding of the
155 underlying processes, scenario-dependence for rapid dynamics could not be
156 established in IPCC AR5.

157

158 Significant progress has been made since then to understand the dynamic processes
159 and quantify their effect on Antarctic ice loss for the 21st century and beyond.
160 Pollard *et al.* [2015] found that crevasse-induced ice shelf loss can lead to the onset
161 of rapid ice discharge from several Antarctic drainage basins. Based on the results
162 from the SeaRISE model intercomparison project [Nowicki *et al.*, 2013], Levermann

163 *et al.* [2014] developed a probabilistic approach to estimate the future sea-level
164 contribution from Antarctica, combining uncertainty in the climatic boundary
165 conditions, the oceanic response and the ice-sheet response. The results, based on
166 linear response theory, correspond with the recently observed mass loss from the
167 Antarctic Ice Sheet [*Shepherd et al.*, 2012]. *Levermann et al.* [2014] find that the 90%
168 uncertainty associated with the contribution from Antarctica reaches up to 0.23 m
169 (median 0.07 m; 90% 0.0-0.23 m) by 2100 for RCP2.6 and up to 0.37 m (median 0.09
170 m; 90% 0.01-0.37 m) for RCP8.5 (Figure 2).

171

172 IPCC AR5 concluded that the collapse of marine ice sheet basins could cause
173 additional SLC above the likely range of ‘up to several tenths of a meter’ [*Church et*
174 *al.*, 2013], but the timing could not be quantified. The mechanism underlying such a
175 potential collapse is the marine ice sheet instability (MISI, *Weertman*, 1974; *Mercer*,
176 1978): several Antarctic basins are partly grounded below sea level, on bedrock
177 generally sloping downwards towards the interior of the ice sheet. If the grounding
178 line retreats into such an area, it could become unstable.

179

180 Shortly after the release of AR5, several studies were published showing with
181 increasing certainty that parts of West Antarctica might in fact already be
182 undergoing unstable grounding line retreat [*Favier et al.*, 2014; *Joughin et al.*, 2014;
183 *Rignot et al.*, 2014]. The retreat was most likely caused by warm circumpolar deep
184 water reaching the ice shelf cavities in recent years – whether this process was
185 influenced by anthropogenic climate change is not yet clear.

186

187 Using a process-based statistical approach, *Ritz et al.* [2015] derived probability
188 estimates for exceeding particular thresholds in the marine basins of Antarctica as a
189 function of time if MISI is triggered. Their results suggest that particularly in the
190 Amundsen Sea Sector, large and rapid ice loss due to the marine ice sheet instability
191 could be initiated within this century. By 2100, the total ice loss from such rapid
192 dynamics is estimated to contribute up to 0.3 m to global SLC, quantifying and
193 narrowing down the IPCC AR5 estimates, and 0.72 m by 2200 (95% quantiles). Large

194 uncertainties remain, especially with respect to the effect of basal sliding on the ice
195 flux [Ritz *et al.*, 2015].

196

197 These advances made in estimating both the gradual response to oceanic warming
198 as well as the possibly abrupt onset of self-sustained grounding line retreat, can be
199 consolidated into a new uncertainty range for Antarctic ice loss. It contains the IPCC
200 likely range but leads to an overall larger spread for the 21st century sea-level
201 projections.

202

203 However, a recent paper by *Pollard and Deconto* [2016] includes a number of
204 processes in their model simulation that were not included in models before, such as
205 the hydrofracturing of Antarctic ice shelves due to atmospheric warming and
206 subsequent ice cliff instabilities. The model is found to be in relatively good
207 agreement with geological estimates of the Pliocene (~three million years ago) and
208 the last interglacial (130,000-115,000 years ago). Depending on the geologic criteria
209 used, they find possible contributions up to 1.05 ± 0.30 m (1σ) by 2100 under the
210 RCP8.5 scenario. This means that the possibility of 1 m SLC from the Antarctic ice
211 sheet still cannot be excluded.

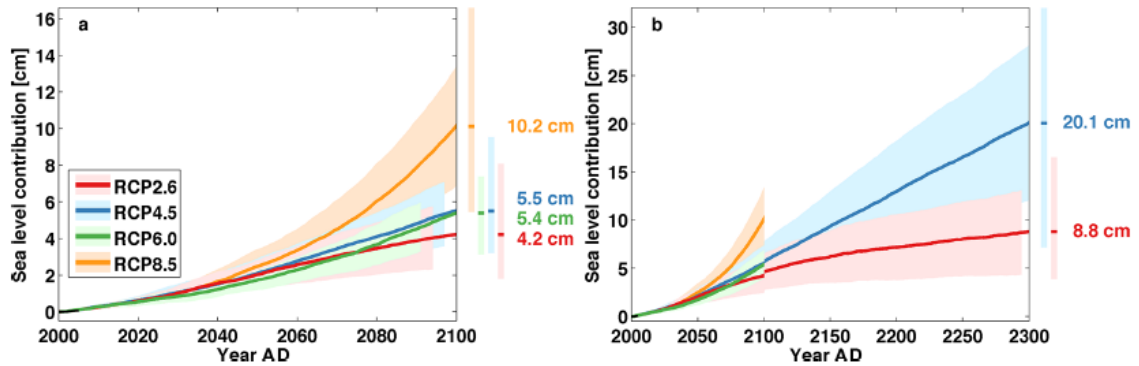
212

213 **Long-term projections** Sea level will continue to rise well beyond 2100, even under
214 strong mitigation scenarios [Church *et al.*, 2013]. Due to the long lifetime of
215 anthropogenic CO₂ in the atmosphere and the consequent slow decline of
216 temperatures, greenhouse gas emissions within this century can induce a sea-level
217 commitment of several meters for the next millennia [Levermann *et al.*, 2013]. On
218 these time-scales the Greenland Ice Sheet shows critical threshold behaviour with
219 respect to atmospheric warming due to the surface-elevation feedback [Ridley *et al.*,
220 2010; Robinson *et al.*, 2012].

221

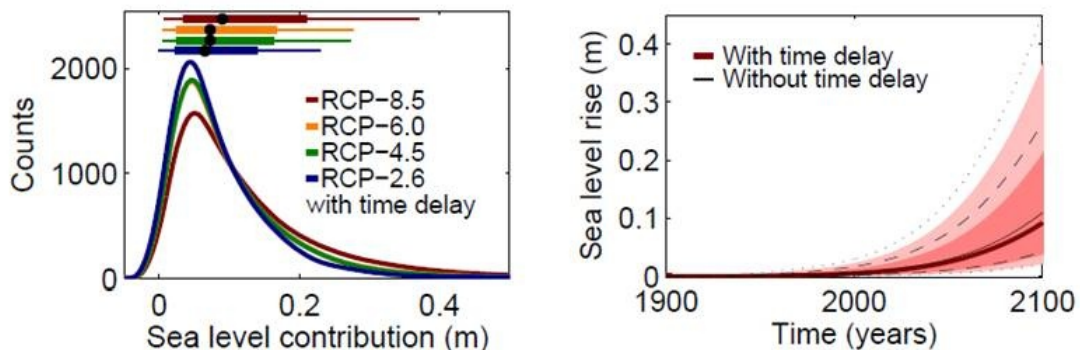
222 Long-term projections from different process-based model simulations are now also
223 available for the Antarctic Ice Sheet [Golledge *et al.*, 2015; Winkelmann *et al.*, 2015].
224 Since several ice basins in Antarctica are potentially pre-conditioned to become
225 subject to MISI, the response of the ice sheet to global warming might also be highly

226 non-linear. *Golledge et al.* [2015] find that the irreversible retreat of major Antarctic
227 drainage basins can only be avoided if greenhouse gas emissions do not exceed the
228 RCP2.6 level. *Winkelmann et al.* [2015] studied the evolution of Antarctica on
229 millennial timescales and show that the West Antarctic ice sheet becomes unstable
230 after 600 to 800 GtC of additional carbon emissions. They further conclude that, on a
231 multi-millennial timescale, Antarctica could become essentially ice-free for a
232 scenario in which all available fossil carbon resources are combusted (10,000 GtC).
233 These new studies suggest that the rate of SLC for higher emission scenarios could
234 reach values of up to a few meters per century beyond 2100.



235

236 Figure 1: Projected global mean sea-level contribution (cm) from the Greenland Ice
 237 Sheet (surface mass balance and dynamics) using a three-dimensional ice flow model
 238 driven by output from 10 atmosphere-ocean general circulation models (a) for four
 239 RCP climate scenarios over the 21st century and (b) for two RCP climate scenarios
 240 until 2300 (reproduced from Fürst et al. [2015]). The shaded area indicates the
 241 ensemble mean $\pm 1\sigma$, while the vertical bars show the spread ($\pm 2\sigma$) at the end of
 242 2100 and 2300 respectively.



243

244 Figure 2: Projected sea-level contribution (m) from the Antarctic Ice Sheet in the 21st
 245 century. (a) Uncertainty range including climate, ocean and ice-dynamic uncertainty
 246 for the year 2100 (top: thick line is 66% range, thin line is 90% range). Different
 247 colours represent different climate scenarios used to drive three Antarctic Ice Sheet
 248 models. (b) Time-series of future SLC from Antarctica (median, 66% and 90%
 249 uncertainty ranges) (reproduced from Levermann et al. [2014]).

250

251 **2.2 Glacier projections**

252 Glacier mass loss constituted a large contributor to 20th century SLC [*Gregory et al.*,
253 2013]. Despite accelerating mass loss of the ice sheets [*Shepherd et al.*, 2012], glacier
254 mass loss continues to be a main component of SLC [*Church et al.*, 2011] and is likely
255 to remain an important factor in the 21st century. The AR5 evaluation of projected
256 glacier mass loss in 2081-2100 relative to 1986-2005 ranges from 0.04 to 0.23 m at
257 2100, based on the results of four process-based models across different forcing
258 scenarios [*Church et al.*, 2013].

259

260 There are five glacier models operating on a global scale which have published
261 projections of glacier mass change under the RCP scenarios [*Marzeion et al.*, 2012;
262 *Hirabayashi et al.*, 2013; *Radić et al.*, 2014; *Slangen et al.*, 2014; *Huss and Hock*,
263 2015] and one study which uses the SRES scenarios to drive their glacier model
264 [*Giesen and Oerlemans*, 2013]. They all combine a glacier surface mass balance
265 model with a model that accounts for the response of glacier geometry to changes in
266 glacier mass. The calculation of both the glacier mass balance and geometry change
267 varies across the different models. All models except *Huss and Hock* [2015] were
268 used in IPCC AR5, but some have been updated since, as will be detailed below.

269

270 *Slangen et al.* [2012, 2014] calculate the glacier mass balance from the sensitivity of
271 the surface mass balance to temperature change and changes in precipitation. This
272 sensitivity is parameterized by relations that are calibrated on more detailed model
273 studies for 12 individual glaciers [*Zuo and Oerlemans*, 1997]. The initial areas of the
274 glaciers are based on WGI-XF (World Glacier Inventory, extended format, *Cogley*
275 [2009]) and the glacier volumes are based on volume area scaling. The glacier
276 projections are forced by 14 models from the CMIP5 database [*Taylor et al.*, 2012a]
277 for each of the RCP4.5 and RCP8.5 scenarios.

278

279 *Radić et al.* [2014] and *Marzeion et al.* [2012] both use an approach in which
280 accumulation and ablation are modelled explicitly. Accumulation is calculated by
281 summing the solid precipitation over the glacier characterized by an area distribution
282 over elevation. Ablation is calculated with a temperature-index method in both

283 studies. Following *Radić and Hock* [2011], *Radić et al.* [2014] calculate the surface
284 mass balance for each glacier at different elevation bands, whereas *Marzeion et al.*
285 [2012] calculate melt from the temperature at the glacier-tongue elevation only.
286 Both studies use mass balance observations to calibrate the modelled glacier mass
287 balance. In order to account for glacier retreat to higher elevations and thus allow
288 for new equilibrium in a different climate, *Radić et al.* [2014] remove, or add in case
289 of modelled mass gain, mass in the lowest elevation bins of the modelled glaciers,
290 based on volume area scaling. *Marzeion et al.* [2012] combine volume-length scaling
291 with the mean slope of the glacier surface to let the glacier terminus retreat to
292 higher elevations, or advance to lower elevations. They also include a response time
293 between volume changes on the one hand, and length and area changes on the
294 other. Their model is validated against in-situ and geodetic mass balance
295 observations of individual glaciers. *Marzeion et al.* [2012] do not model peripheral
296 glaciers (PGs) in Antarctica explicitly, but apply the global mean specific mass
297 balance rate as a rough approximation.

298

299 The results of *Radić et al.* [2014] shown in Figure 3 are from projections that are
300 forced by 14 models from the CMIP5 database for each of the RCP4.5 and RCP8.5
301 scenarios. The results of *Marzeion et al.* [2012] were updated based on a more
302 recent version of the Randolph Glacier Inventory (RGI). Their projections were forced
303 by 13 CMIP5 models for the RCP2.6 scenario, 15 models for RCP4.5, 11 models for
304 RCP6.0 and 15 models for RCP8.5.

305

306 *Huss and Hock* [2015] use a temperature-index model to calculate mass changes for
307 every individual glacier, but their model approach is different from the earlier
308 models discussed above concerning a few points. They do not use volume-area or
309 volume length scaling. Instead they derive the initial glacier volume following *Huss*
310 *and Farinotti* [2012]. This method provides ice thickness, and therefore glacier
311 volume and glacier bed elevation, distributed over 10 m elevation intervals for every
312 glacier. Glacier geometry changes due to changes in calculated glacier mass are
313 distributed over the glacier elevation following the parameterization of *Huss et al.*
314 [2010]. Furthermore, *Huss and Hock* [2015] explicitly compute mass loss through

315 calving using the simple model of *Oerlemans and Nick* [2005] that describes the
316 calving rate as a linear function of the height of the calving front. Finally, they
317 subtract the mass loss of glacier ice below sea level, which does not contribute to
318 SLC, from the total of calculated glacier mass loss in their calculation of the glacier
319 contribution to SLC (note that for comparability, the loss of ice below sea level is also
320 included in their numbers shown in Figure 3). For calibration, *Huss and Hock* [2015]
321 assume that mean specific balance rate of each individual glacier should equal the
322 observed region-wide mean specific balance rate [*Gardner et al.*, 2013] within a
323 range of ± 0.1 m w.e.a⁻¹. The model is validated against in-situ and geodetic mass
324 balance observations, as well as observed area changes and calving rates, for
325 individual glaciers. The results of *Huss and Hock* [2015] used here are from
326 projections that are forced by 12 models from the CMIP5 database for the RCP2.6
327 scenario and 14 models for the RCP4.5 and RCP8.5 scenarios.

328

329 *Hirabayashi et al.* [2013] use a grid-based approach to modeling glacier mass change.
330 Within each 0.5 x 0.5 degree grid cell, individual glaciers are lumped together as one
331 glacier, while applying sub-gridscale elevation bands preserves the vertical elevation
332 distribution of the ice area within each grid cell. Their model was calibrated against
333 the observations of *Dyurgerov and Meier* [2005] and does not cover PGs on
334 Greenland or Antarctica. The projections used here are forced by 10 models from
335 the CMIP5 database for the RCP8.5 scenario only.

336

337 In each of the five global studies described above, the mass balance is calculated
338 with a temperature-index model. *Giesen and Oerlemans* [2013] apply a more
339 complex surface mass balance model that besides the dependence of glacier mass
340 balance on temperature and precipitation also includes incoming solar radiation in
341 the calculation of ablation. They calibrate this model to 89 glaciers with in-situ
342 observations of winter and summer mass balance and then upscale the results to all
343 glaciers. Their projections for the 21st century are based on an ensemble of CMIP3
344 model runs for scenario A1B. They find a significant effect of projected decrease in
345 incoming solar radiation in the Arctic region on the projected sea-level contribution.
346 The 21st century global glacier mass loss found in *Giesen and Oerlemans* [2013] is

347 significantly less than in other studies [*Marzeion et al.*, 2012; *Radić et al.*, 2014;
348 *Slangen et al.*, 2014] for comparable RCPs. In a regional study of future surface mass
349 balance with the high resolution regional climate model MAR, *Lang et al.* [2015] find
350 significantly less mass loss for Svalbard than *Marzeion et al.* [2012] and *Radić et al.*
351 [2014]. Suggested explanations for this discrepancy are the coarse resolution of the
352 global climate models that were used to force the global glacier models, and a better
353 representation of the physical processes in the regional climate model compared to
354 the empirical temperature-index mass balance models. *Lang et al.* [2015] also find a
355 significant reduction of the incident solar radiation due to increased cloudiness,
356 supporting the findings of *Giesen and Oerlemans* [2013] for the Arctic. *Huss and*
357 *Hock* [2015] also find a 16-22% lower projected glacier mass loss when they include
358 incoming solar radiation (assumed to be constant in time) in a sensitivity experiment
359 with their glacier mass balance model.

360

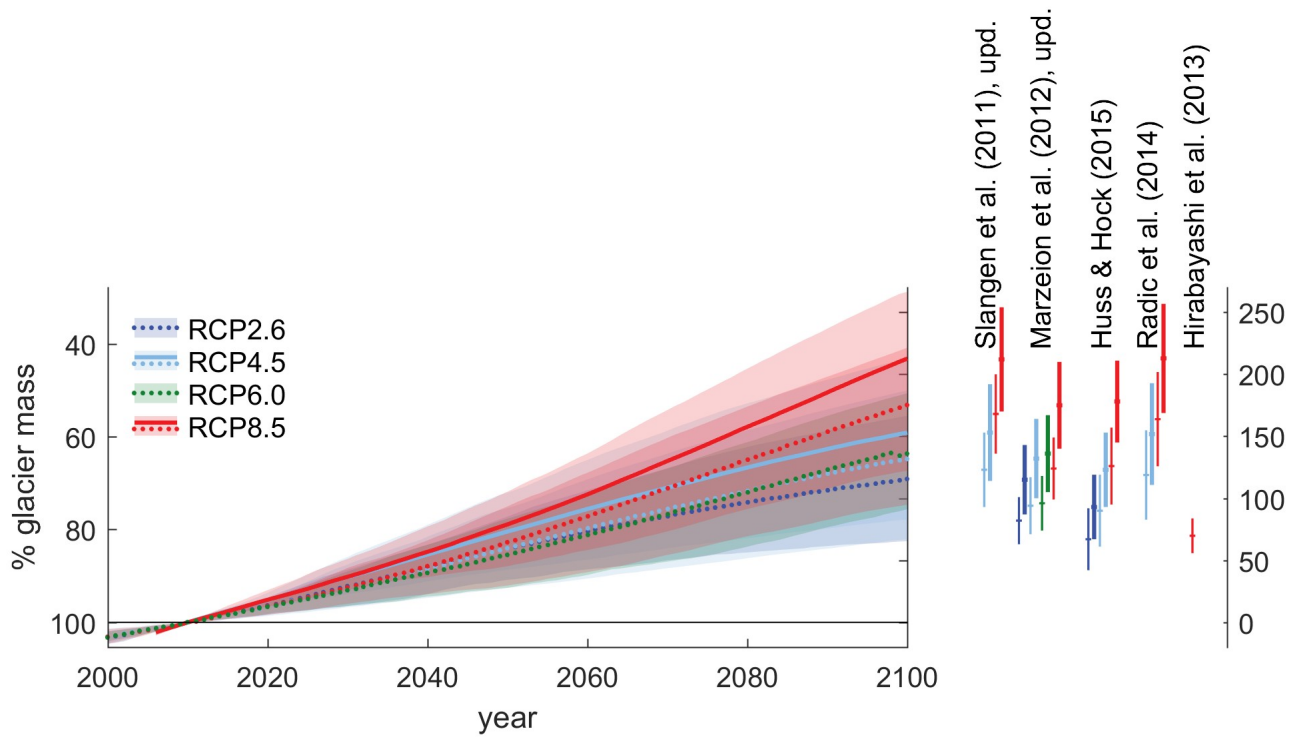
361 Figure 3 shows the projected glacier mass loss from the 5 global studies under RCP
362 scenarios. They all show a large spread in the projected global glacier mass loss
363 within the ensemble of different climate model runs for the same scenario. The
364 ensemble standard deviation within each scenario is comparable to the differences
365 between the ensembles means of different scenarios. Also the differences between
366 the different glacier models, but identical scenarios, are of comparable magnitude.
367 The exception is the projection of *Hirabayashi et al.* [2013], which for the RCP8.5
368 scenario projects glacier mass loss comparable to the other models' projections for
369 RCP2.6.

370

371 Updates of existing projections [*Marzeion et al.*, 2012] and new models [*Huss and*
372 *Hock*, 2015] published after the IPCC AR5 have generally lead to slightly lower
373 projected mass losses (Table 1). For the RCP8.5 scenario for instance, IPCC AR5
374 projected a contribution of 16 ± 7 cm, while *Huss and Hock* [2015] and the updated
375 *Marzeion et al.* [2012] present projections around 12.5 cm for the same scenario. In
376 the case of *Marzeion et al.* [2012] this is attributable to updates of the RGI; it is
377 unclear for *Huss and Hock* [2015] since no previous estimate existed. On the other
378 hand, the results of *Slangen et al.* [2012, 2014] are very similar to *Radić et al.* [2014].

379 The results of *Giesen and Oerlemans* [2013] and *Lang et al.* [2015] suggest that a
380 projected decrease in Arctic incoming solar radiation could lead to a lower projected
381 mass loss than is given by the temperature index models. However, a direct
382 comparison of the individual studies is complicated through the differing
383 compositions of the ensembles used for forcing the glacier models. Therefore, a
384 coordinated glacier model intercomparison is currently underway to better
385 understand the causes of the model and ensemble spread.

386



387

388 Figure 3: Projected global mean sea-level contribution from glacier mass loss. Left
 389 panel: Percentage of glacier mass remaining (%), ensemble mean (lines) and 1 σ
 390 spread (shading), dashed lines excluding, full lines including peripheral glaciers on
 391 Greenland and Antarctica. Right panel: glacier contribution to SLC by 2100 (mm),
 392 ensemble mean and 1 ensemble standard deviation in 2100; thick lines including,
 393 thin lines excluding peripheral glaciers. All numbers are relative to 2010.

394 Table 1: Projected glacier contributions to SLC for 2010-2100 (mm, ensemble mean $\pm 1 \sigma$),
 395 for four different RCP scenarios, peripheral glaciers excluded (numbers in brackets include
 396 peripheral glaciers).

Study	RCP2.6	RCP4.5	RCP6.0	RCP8.5
[Hirabayashi et al., 2013]	-	-	-	73 \pm 14
[Huss and Hock, 2015]	67 \pm 25 (93 \pm 26)	90 \pm 29 (123 \pm 30)	-	126 \pm 31 (178 \pm 33)
[Marzeion et al., 2012, upd]	82 \pm 19 (115 \pm 28)	94 \pm 23 (132 \pm 32)	96 \pm 22 (136 \pm 31)	124 \pm 25 (175 \pm 35)
[Radić et al., 2014]	-	122 \pm 36 (155 \pm 41)	-	167 \pm 38 (216 \pm 44)

[<i>Slangen and van de Wal</i> , 2011, upd]	-	123 ± 30 (153 ± 39)	-	168 ± 32 (212 ± 42)
-------------------------------------------------	---	------------------------	---	------------------------

397

398 3. Terrestrial water storage change projections

399 Terrestrial water storage (TWS) change can result in a positive contribution to SLC
400 due to a net transfer of water from long-term groundwater storage to the active
401 hydrological cycle and eventually to ocean storage [Gornitz, 1995; Taylor et al.,
402 2012b]. Other terrestrial components potentially contributing to SLC include water
403 impoundment behind dams (which can cause sea-level fall), drainage of endorheic
404 lakes (mostly from the Aral Sea) and wetlands, deforestation, and changes in natural
405 water storage (soil moisture, groundwater, permafrost and snow). Natural TWS
406 change mostly varies with decadal climate variation with no significant trend.

407

408 *Chao et al.* [2008] found that the volume of water accumulated in dams up to 2010 is
409 equivalent to a sea-level fall of ~30 mm. However, *Lettenmaier and Milly* [2009]
410 indicated that the volume of silt accumulated in dams should be removed from the
411 estimate, which is equal to ~4 mm less sea-level fall. Indeed, silting-up of existing
412 dams may already be, or in coming decades may become, a larger effect on
413 impoundment than construction of new dam capacity [*Wisser et al.*, 2013].

414

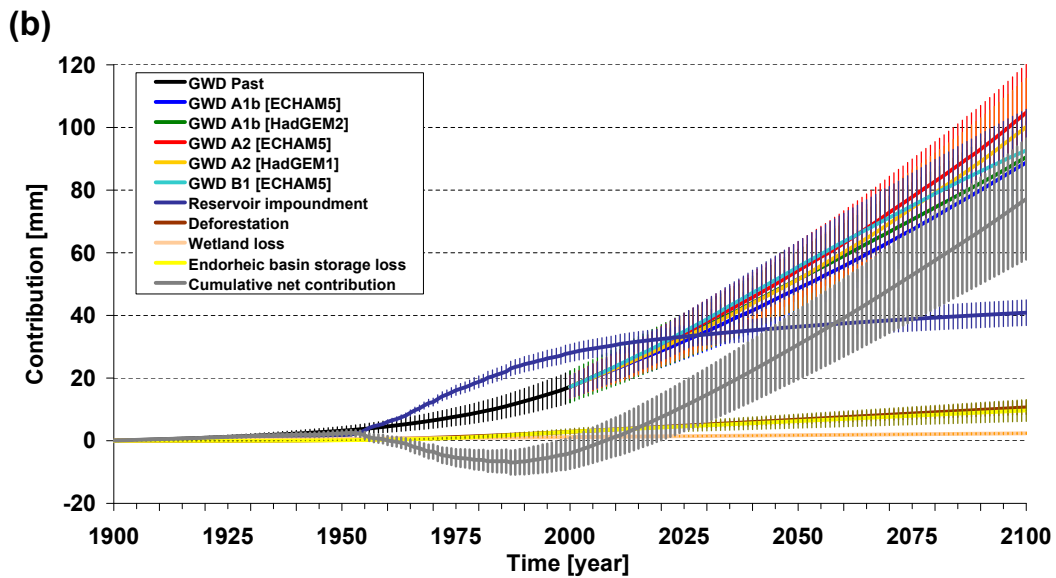
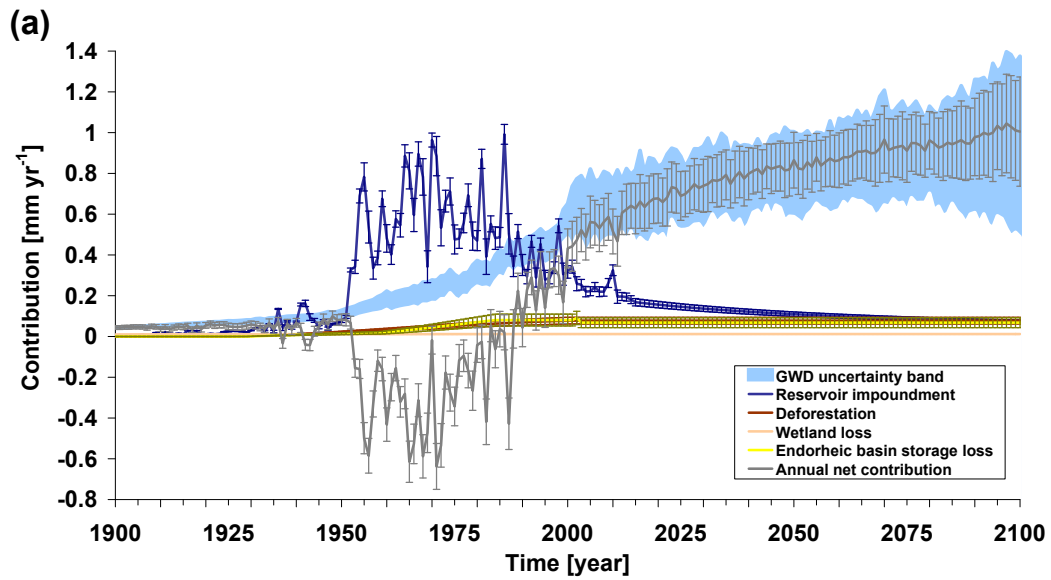
415 Using a global hydrological model, *Wada et al.*, 2012 estimated that the contribution
416 of groundwater depletion (GWD) to SLC increased from 0.035 ± 0.009 mm yr⁻¹ in
417 1900 to 0.57 ± 0.09 mm yr⁻¹ in 2000 (Figure 4). These figures were recently revised to
418 lower values in *Wada et al.* [2016], who found a sea-level contribution of 0.12 ± 0.04
419 mm yr⁻¹ for the period 1993-2010 using a coupled climate-hydrological model. A
420 volume-based study by *Konikow* [2011] also found slightly lower values than *Wada*
421 *et al.* [2012] using direct groundwater observations, calibrated groundwater
422 modelling, GRACE satellite data, and partly extrapolation for some regions. Also
423 combining hydrological modelling with information from well observations and
424 GRACE satellites, *Döll et al.* [2014] estimated the SLC contribution of GWD was 0.31
425 mm yr⁻¹ during 2000-2009. Another study [*Pokhrel et al.*, 2012] used an integrated
426 water resources assessment model to estimate all changes in TWS. However, their
427 estimate is likely to overestimate the GWD contribution, because the model did not
428 account for any physical constraints on the amount of groundwater pumping.

429

430 Satellite observations have opened a path to monitor groundwater storage changes
431 in data scarce regions [Famiglietti, 2014]. Since its launch in 2002, the GRACE
432 satellite has been increasingly employed to quantify GWD at regional scales [Rodell
433 *et al.*, 2009; Famiglietti *et al.*, 2011]. GWD can be assessed after subtracting
434 remaining TWS changes from GRACE-derived total TWS changes. However, coarse
435 spatial resolution and noise contamination inherent in GRACE data hinder their
436 global application in estimating GWD [Longuevergne *et al.*, 2010].

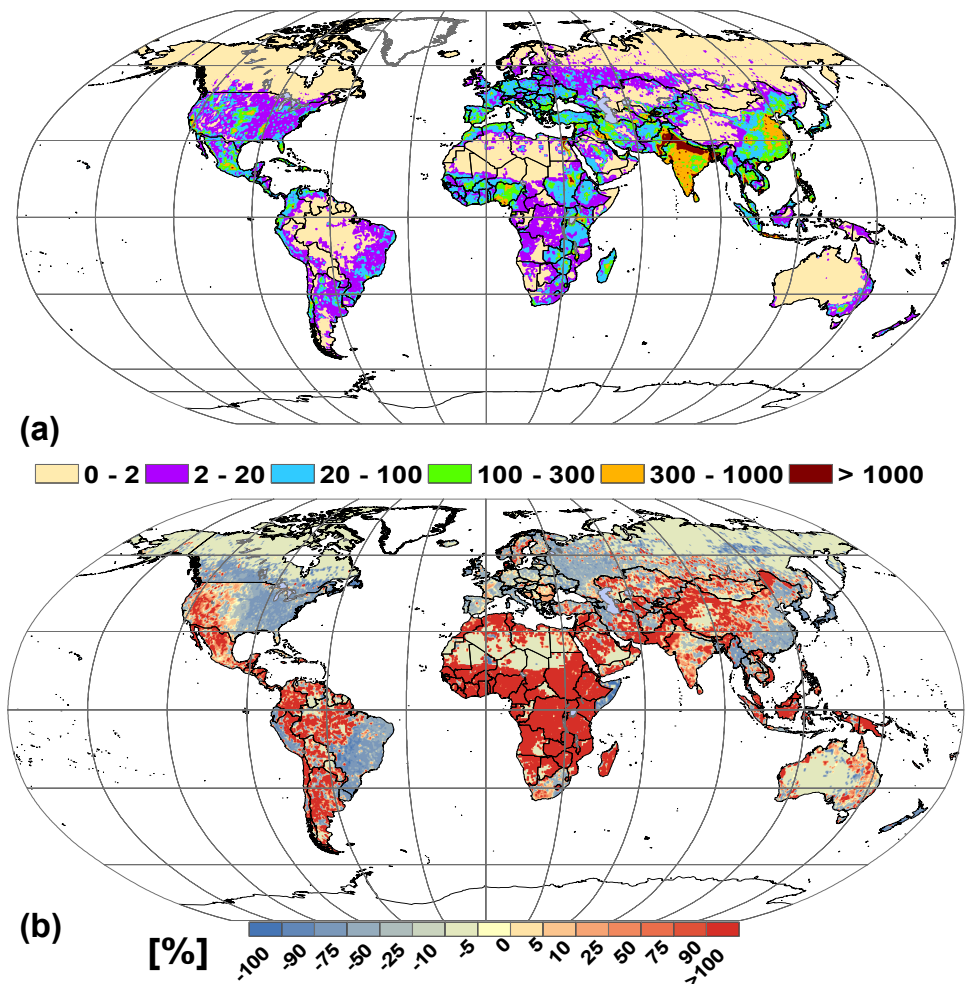
437

438 Future projections of the GWD contribution to SLC are subject to large uncertainties
439 due to the combination of climate projections from AOGCMs with future socio-
440 economic and land use scenarios that are inherently uncertain. The TWS
441 contribution to SLC is projected to be 38.7 ± 12.9 mm, based on CMIP3 climate
442 model output [Wada *et al.*, 2012; Church *et al.*, 2013]. Since IPCC AR5, the
443 groundwater model simulation has been updated, based on the latest CMIP5 climate
444 and IPCC AR5 socio-economic datasets (see Figure 5 for the latest projection of
445 human water consumption from [Wada and Bierkens, 2014]), but does not provide
446 the GWD contribution to SLC yet. The existing 21st century projections indicate
447 increasing GWD caused by (1) increasing water demand due to population growth
448 and (2) an increased evaporation is projected in irrigated areas due to changes in
449 precipitation variability and higher temperatures. Groundwater depletion will be
450 limited by decreasing surface water availability and groundwater recharge, which
451 may cause groundwater resources to become exhausted at some time in the coming
452 century [Gleeson *et al.*, 2015].



453
 454 Figure 4: Historical and projected terrestrial water contributions to SLC for a range of
 455 processes. (a) yearly rates for 1900-2100 (mm yr^{-1}) and (b) cumulative contribution
 456 to SLC wrt 1900 (mm). Bars indicate 1σ standard deviation. Blue band in (a) is based
 457 on 10,000 Monte Carlo realisations from 5 future projections of groundwater

458 depletion, individual projections and uncertainties shown in (b) (from *Wada et al.*
459 [2012]).
460



461
462 Figure 5: (a) Projected global human water consumption in 2099 (million m³ yr⁻¹) and
463 (b) the relative change (%) between 2010 and 2099 (From *Wada and Bierkens*
464 [2014]).
465

466 **4. Global mean sea-level projections**

467 Before we discuss total global mean sea-level projections, we briefly discuss thermal
468 expansion, as this is one of the most important contributors to global mean sea-level
469 change. The majority of the net energy increase in the Earth's climate system is
470 stored in the ocean, increasing the ocean heat content, which leads to warming and
471 expansion of the ocean water. The resulting global mean thermosteric SLC by 2100 is
472 projected to be 0.14 m (\pm 0.04 m) for the RCP2.6 scenario, up to 0.27 m (\pm 0.06 m)
473 for the RCP8.5 scenario in IPCC AR5 [*Church et al., 2013*]. New results are expected
474 when the output of the sixth Climate Modelling Intercomparison project is released
475 from 2017 onwards.

476

477 Although the focus in sea-level science is gradually moving towards regional SLC
478 projections, as this is more relevant for coastal adaptation, there are still lessons to
479 be learnt from the global mean SLC. The signal-to-noise ratio is smaller in the global
480 mean, allowing a focus on long-term changes rather than local, short-term
481 variability. As a result, it can be used to focus on narrowing uncertainties in the
482 projections.

483

484 A notable development in global mean sea-level projections since IPCC AR5 is the
485 use of a probabilistic approach to explore uncertainties in sea-level projections
486 beyond the likely range [*Jevrejeva et al., 2014; Kopp et al., 2014; Grinsted et al.,*
487 *2015*]. In this approach, the projections (as presented in IPCC AR5) are blended with
488 expert assessments of the Greenland and Antarctic ice sheet contributions [*Bamber*
489 *and Aspinall, 2013*] or expert assessments of total SLC [*Horton et al., 2014*]. Expert
490 assessments of, for instance, the potential contribution from ice sheets can be a
491 useful tool to assess the uncertainty ranges, because the ice sheet experts know
492 which particular physical processes (e.g. calving, ice sheet-ocean interaction) are
493 insufficiently represented in their ice sheet models. One should keep in mind
494 however that the current changes in the climate system are unprecedented and
495 estimates based on intuition, such as expert assessments, should therefore be used
496 with care.

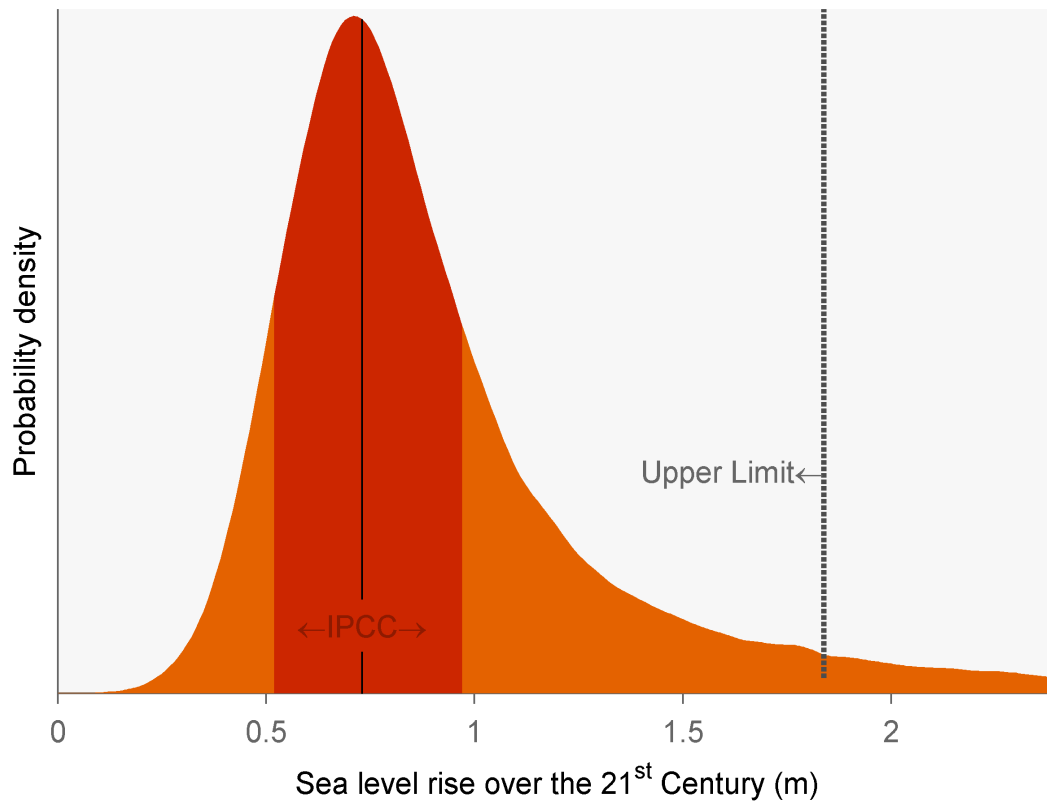
497

498 Figure 6 demonstrates the difference between the conventional and probabilistic
499 approaches for global sea-level projections. Probabilistic projections allow the
500 selection of specific probability levels to estimate low-probability/high-risk SLC
501 projections, which by definition are unlikely to be reached, but cannot be ruled out
502 given paleoclimate proxy information and the limitations in process based modelling
503 [Jevrejeva *et al.*, 2014]. They also allow for the use of probability distributions that
504 do not follow a Gaussian distribution, such as skewed probability distributions with a
505 longer tail to high SLC projections (Figure 6).

506

507 In addition to the studies focusing on uncertainties in the global mean, a new
508 application of the semi-empirical approach was published recently by *Mengel et al.*
509 [2016]. Semi-empirical models were developed after IPCC AR4 to offer an alternative
510 to more complicated physical models of SLC. They are based on the assumption that
511 sea level in the future will respond to imposed climate forcing as it has in the past,
512 which may not hold if potentially non-linear physical processes, such as marine ice-
513 sheet instability or thermal expansion, do not scale in the future as they have in the
514 past. *Mengel et al.* [2016] calibrate the semi-empirical model for each contribution
515 separately, such that the timescales of each contribution are considered in the
516 calibration of the model. Their projected global mean SLC by 2100 is 84.5 cm (57.4-
517 131.2 cm; median, 5th and 95th percentile) under the RCP8.5 scenario. This brings the
518 semi-empirical models closer to the process-based IPCC AR5 estimates of 74 cm (52-
519 98 cm) than other, larger, semi-empirical estimates at the time of IPCC AR5 [*Church*
520 *et al.*, 2013, Table 13.6].

521



523

524 Figure 6: Projected global mean sea-level rise by 2100 relative to 2000 for the RCP8.5
525 scenario and uncertainty (m). Dark orange represents the mean (black line) and likely
526 range from IPCC AR5 [Church et al., 2013], light orange represents the probabilistic
527 uncertainties from Jevrejeva et al. [2014]. The vertical dotted black line represents
528 the 95% probability estimate of sea-level rise in 2100 (1.8 m). (from Jevrejeva et al.
529 [2014])

530

531 5. Regional sea-level projections

532 Regional SLC can deviate substantially from the global mean due to a number of
533 processes. Firstly, oceanic and atmospheric circulation changes and heat and salt
534 redistribution in the ocean change the density of the water as well as redistribute
535 mass within the oceans [Yin *et al.*, 2010; Yin, 2012]. Secondly, any redistribution of
536 mass between ocean and land, such as land ice mass change or TWS, affects the
537 gravitational field of the earth and causes visco-elastic deformation of the Earth's
538 crust, the combination of which results in distinct sea-level patterns referred to as
539 'fingerprints' [Farrell and Clark, 1976; Mitrovica *et al.*, 2001]. Thirdly, regional sea
540 level can be influenced by vertical land motion, such as tectonic activity or Glacial
541 Isostatic Adjustment (GIA). GIA is the present-day viscous deformation of the Earth's
542 crust as a result of ice melt after the Last Glacial Maximum, which in turn also affects
543 the gravitational field [Peltier, 2004]. GIA can have large local effects, while on a
544 global mean scale the effect is negligible.

545

546 IPCC AR5 [Church *et al.*, 2013] adopted the approach from Slangen *et al.* [2012,
547 2014] to compute regional sea-level projections by combining climate model results
548 for thermal expansion and circulation changes with offline models to compute
549 gravitational fingerprints as a result of mass change and GIA. Using this approach,
550 both IPCC AR5 and Slangen *et al.* [2014] project regional sea-level values up to 20%
551 larger than the global mean in equatorial regions (Figure 7), while close to regions of
552 ice mass loss the values can be as small as 50% of the global mean, mainly as a result
553 of the gravitational effect. The meridional dipole in the Southern Ocean and the
554 dipole in the North Atlantic are associated with the response of dynamic sea level
555 (DSL) to increasing greenhouse gas forcing [Bilbao *et al.*, 2015; Slangen *et al.*, 2015],
556 through wind stress and surface heat flux changes [Bouttes and Gregory, 2014].

557

558 Carson *et al.* [2015] used the regional projections from Slangen *et al.* [2014] to study
559 coastal SLC and found that coastal deviations from the global mean by 2100 can be
560 up to 20 cm. The same regional sea-level projections were also used for a number of
561 national assessments, such as Simpson *et al.* [2014] in Norway and Han *et al.* [2014,
562 2015] in Canada, where the global GIA model estimates were corrected or replaced

563 by more accurate local GIA models or GPS measurements. Other regional
564 assessments were done in e.g. Australia [CSIRO and Bureau of Meteorology, 2015;
565 *McInnes et al.*, 2015] and the Netherlands [*Vries et al.*, 2014], which build on the
566 IPCC-type regional sea-level projections. However, to really make a step forward in
567 these national assessments, finer grid resolutions will be required to improve the
568 model representation of ocean dynamical processes.

569

570 Using a probabilistic approach, *Kopp et al.* [2014] combined climate model
571 information with an expert elicitation of the ice sheet contributions [*Bamber and*
572 *Aspinall*, 2013] to provide complete probability distributions of regional SLC
573 projections. While the mean SLC is similar to IPCC AR5, *Kopp et al.* [2014] present
574 high-end estimates which can be of particular interest and relevance for coastal
575 management purposes. Following onto this, *Little et al.* [2015a] combined
576 probability distributions with statistical models to estimate coastal flooding risk due
577 to storm surges and SLC. They found that the risk of floods at the US East coast
578 substantially increases as a result of SLC and changes in the frequency and intensity
579 of tropical cyclones. However, these results were based on SLC from climate models
580 only and do not include the SLC as a result of land-ice melt or TWS, which could lead
581 to even larger flood risks.

582

583 To study the sources of uncertainty in sea level from climate models, *Little et al.*
584 [2015b] decomposed the uncertainty into several components: model uncertainty,
585 internal variability, scenario uncertainty and a model-scenario interaction
586 component. They found that in the global mean, model uncertainty is the dominant
587 term in the variance, whereas the variance due to scenario uncertainty increases in
588 the 21st century and variance due to internal variability is initially large but decreases
589 quickly. Locally, the contribution of each source of uncertainty can be very different,
590 depending on the local magnitude of internal variability versus the response to
591 external climate forcings. Both *Hu and Deser* [2013] and *Bordbar et al.* [2015]
592 showed that internal variability in some locations can even be sufficiently large to be
593 the main source of uncertainty all through the 21st century. As a result of the large
594 internal variability, the time of emergence of SLC for DSL only [*Lyu et al.*, 2014, their

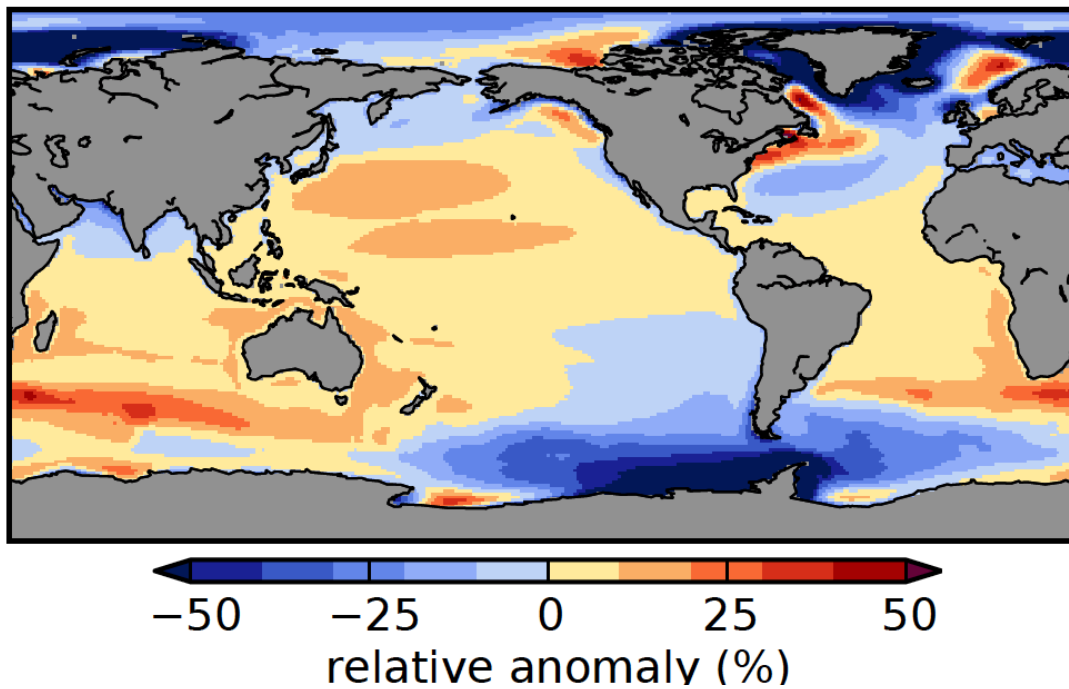
595 Figure 2a) is beyond 2100 for over 80% of the ocean area. The area with an emerging
596 signal increases significantly (to almost 100% by 2080) when thermal expansion, land
597 ice, GIA and GWD are included. For a further discussion of literature on the effect of
598 unforced variability on sea level and detection and attribution of SLC, see Han et al.
599 and Marcos et al. in this issue, respectively.

600

601 The effect of freshwater input into the ocean as a result of land ice mass loss has
602 been discussed in a number of studies, which have produced climate projections
603 with integrated realistic estimates for glacier and ice sheet melt water runoff
604 [*Howard et al.*, 2014; *Agarwal et al.*, 2015; *Lenaerts et al.*, 2015]. The first two
605 studies focus on the impact of the freshwater forcing on DSL and find, using different
606 models and different scenario's, that the impact is small (in the order of several cm)
607 compared to the total SLC projected for the 21st century. However, both *Howard et*
608 *al.* [2014] and *Lenaerts et al.* [2015] find that adding ice sheet freshwater forcings
609 leads to a slight weakening of the Atlantic Meridional Overturning Circulation,
610 indicating that it is important to include the freshwater forcing in climate models.

611

612



613

614 Figure 7: Relative regional sea-level anomaly from the global mean change (over
615 1986-2005 and 2081-2100, %), based on the CMIP5-RCP4.5 scenario. (From *Slangen*
616 *et al.* [2014]).

617

618 **6. Mediterranean sea-level projections**

619 The Mediterranean is a semi-enclosed basin, linked to the open ocean through the
620 strait of Gibraltar. The high population density at the coast makes this basin
621 particularly vulnerable to future SLC. Mediterranean sea level is influenced by
622 various complex processes such as mass fluctuations (e.g. additional water input),
623 variation in the density structure (steric effect), changes in circulation, waves,
624 atmospheric pressure variations and changes in the hydrographic conditions of
625 incoming Atlantic water. These different components contribute to SLC at different
626 time scales, from daily to interdecadal.

627

628 So far, global climate modelling attempts to assess future SLC in the Mediterranean
629 did not deliver a consistent signal. *Marcos and Tsimplis* [2008] used projections from
630 IPCC models to assess the interannual variation of steric sea level averaged for the
631 Mediterranean, under the SRES A1B scenario, and found that global models do not
632 agree on a trend. Indeed, their coarse resolution does not enable an accurate
633 representation of important small-scale processes acting in the Mediterranean
634 region, which are important to represent the water masses of the basin accurately.
635 Additionally, AOGCM's have difficulties to simulate a reasonable water exchange at
636 Gibraltar, which strongly influences the circulation and the changes in sea level in
637 the Mediterranean Sea.

638

639 High resolution regional climate modelling is thus needed to answer the question of
640 ongoing Mediterranean SLC [*Calafat et al.*, 2012]. In addition to the thermosteric
641 component, the contribution from changes in salinity has to be taken into account
642 for the Mediterranean, since climate projections predict that the basin will become
643 saltier in the future. *Jordà and Gomis* [2013] underlined that the saltening of the
644 Mediterranean has two counteracting effects on sea level. Firstly, the halosteric
645 effect leads to contraction of the water and thus a sea-level fall (-0.10 mm yr^{-1} for
646 1960-2000). In contrast, the addition of salt to the basin in terms of mass leads to a
647 sea-level rise ($+0.12 \text{ mm yr}^{-1}$ for 1960-2000). As a simplification, these two
648 contradicting effects can be neglected and Mediterranean mean SLC can be
649 restricted to its thermosteric component.

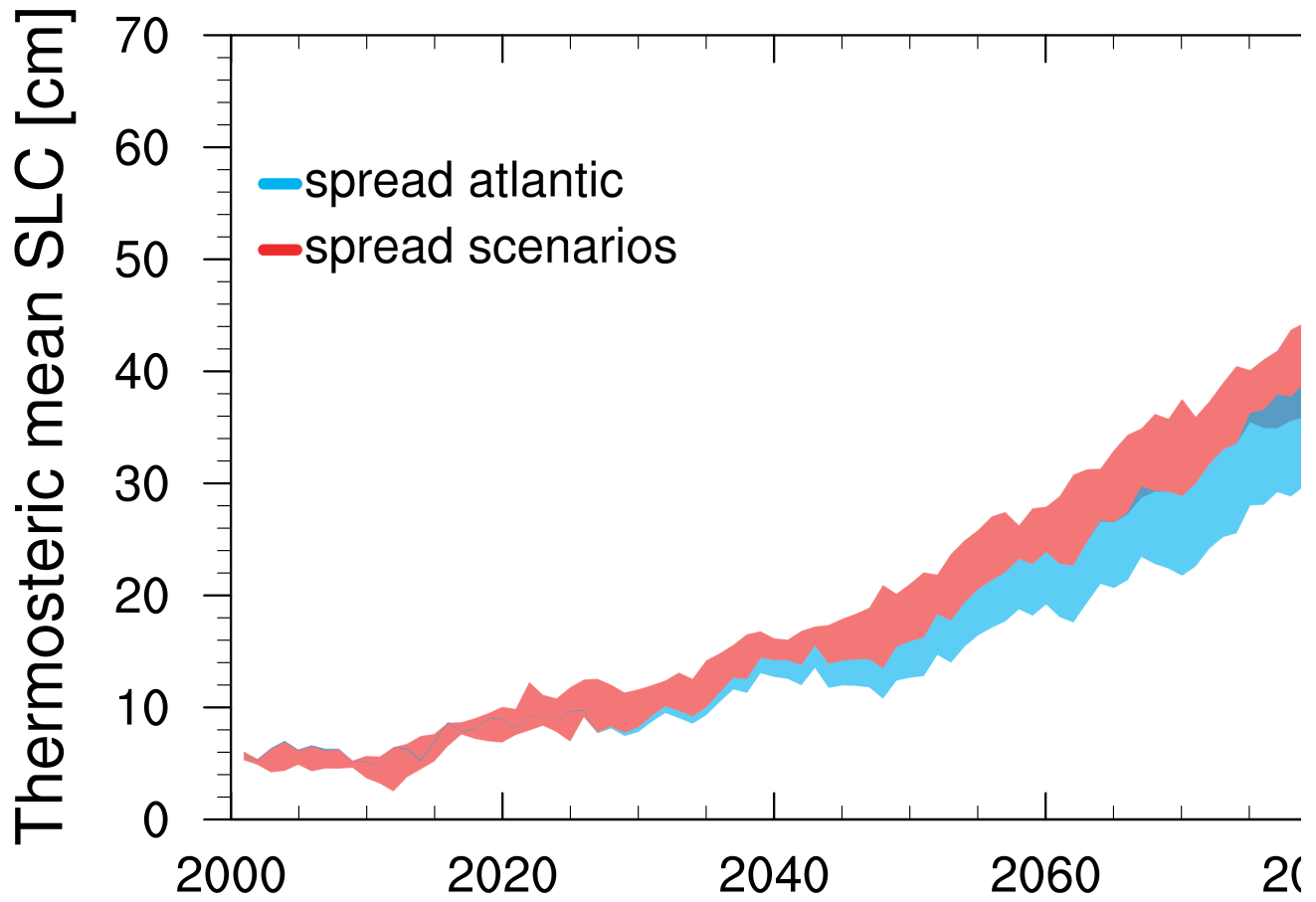
650

651 Two recent studies have analysed Mediterranean SLC in future scenarios with
652 regional models. *Carillo et al.* [2012] projected a thermosteric sea-level rise from 5 to
653 7 cm by 2050 (vs. 1951-2000) for the A1B scenario. With a 6-member ensemble of
654 scenario simulations, *Adloff et al.* [2015] found a larger sea-level rise of 10-20 cm in
655 2050 and 45-60 cm in 2099 (with respect to 1961-1990). In both studies, a large
656 source of uncertainty is attributed to the hydrographic characteristics of the Atlantic
657 boundary conditions prescribed in the Mediterranean model. Using the ensemble of
658 *Adloff et al.* [2015], Figure 8 shows the comparison of the spread of thermosteric
659 sea-level response of the Mediterranean linked to (1) the choice of hydrographic
660 conditions of Atlantic waters prescribed at the western boundary of the
661 Mediterranean, and (2) the choice of the socio-economic scenario. These results
662 confirm how much the Mediterranean response in the future is driven by the
663 Atlantic behaviour and raises the importance of the dataset (mostly AOGCM-
664 derived) used to force the regional model at the boundary with the open ocean.
665 Keeping in mind that the range of changes in near-Atlantic hydrography explored in
666 the study by *Adloff et al.* [2015] is much smaller than the spread among CMIP
667 models, it only gives a lower bound for the range of uncertainties in Mediterranean
668 sea-level projections.

669

670 In comparison to the significant progress at the global scale, the advances at the
671 Mediterranean scale remain small in terms of sea-level representation in regional
672 ocean models. There is a significant lack of regional studies dealing with
673 Mediterranean sea level, for hindcast periods as well as for projections, and none of
674 them account for a proper Atlantic sea-level signal. The next step would be to
675 include this missing feature and prescribe the complete sea-level signal at the
676 Atlantic western boundary of Mediterranean regional models. This would allow to
677 account for the correct evolution of the Atlantic ocean, which pilots part of the
678 Mediterranean behaviour.

679



680

681 Figure 8: Cumulative thermosteric sea level change w.r.t. 1961-1990 (cm), averaged
 682 over the Mediterranean Sea from the 6-member ensemble scenario simulations
 683 from *Adloff et al.* [2015]. In blue the uncertainties linked to the choice of the
 684 prescribed hydrographic conditions of Atlantic waters west of Gibraltar, in red the
 685 uncertainties linked to the choice of the socio-economic scenario.

686

687 **7. Synthesis**

688 The field of sea-level research and all of its contributions is moving quickly, and a lot
689 of work has been done since IPCC AR5. Here, we have reviewed recent literature of
690 projected sea-level contributions of ice sheets, glaciers and terrestrial water storage
691 to sea-level change. Furthermore, we discussed recent advances in global, regional
692 and Mediterranean sea-level projections. We did not discuss contributions that have
693 seen little progress since IPCC AR5, most notably the thermal expansion and ocean
694 dynamics components. However, these components are expected to be updated
695 once the new model runs of the sixth phase of the Climate Model Intercomparison
696 Project (CMIP6) become available.

697

698 The most recent sea-level projections for the Greenland ice sheet of 0.01-0.17 m by
699 2100 largely fall within the IPCC AR5 likely range for the 21st century. However, the
700 contribution of surface melting is larger and the contribution of dynamic discharge is
701 smaller than in IPCC AR5. Most projections for the Antarctic Ice Sheet since IPCC AR5
702 limit the sea-level contribution to 0.3 m by the end of this century as a result of
703 dynamic discharge and the potential onset of the marine ice-sheet instability. All
704 processes combined, the 90% uncertainty of the Antarctic contribution to SLC
705 reaches up to 0.37 m by 2100 under the RCP8.5 scenario. However, a recent
706 publication challenges this and projects changes of well over 1 m by 2100 under the
707 RCP8.5 scenario. All publications project that the bulk of SLC from Greenland and
708 Antarctica will however occur after 2100 and might surpass several meters within
709 the next centuries to millennia.

710

711 Glacier mass loss has been one of the main contributors to sea-level rise in the 20th
712 century and is expected to remain an important contributor in the next century. The
713 latest findings, based on updates of glacier outlines used in existing projections and
714 also new glacier models, project slightly lower contributions to sea-level rise from
715 glaciers compared to IPCC AR5: from projections around ~0.16 m in IPCC AR5 to
716 ~0.12-0.13 m for the RCP8.5 scenario in more recent publications.

717

718 The sea-level contribution of changes in terrestrial water storage (TWS) has been
719 difficult to estimate from observations in the past, but satellite observations now
720 allow for better monitoring of changes in land water storage. Groundwater depletion
721 is projected to increase due to growing water demand as a result of population
722 growth and increasing evaporation. The projected contribution of TWS is 38.7 ± 12.9
723 mm for the period 2010-2100 (ensemble mean $\pm 1 \sigma$).

724

725 In projecting global mean SLC, the focus has turned towards providing better
726 uncertainty estimates by using probabilistic methods and skewed uncertainty
727 distributions. This may lead to better estimates of the low-probability/high-risk
728 events in a changing climate. So far, these improved uncertainty distributions are
729 based on expert elicitations, but as models evolve hopefully the uncertainty
730 estimates will be based on modelling of physical processes in the near future.

731

732 Although significant advances have been made in recent years in projecting regional
733 SLC, there are still a number of challenges that remain. The modelling and
734 understanding of the ocean dynamical processes and incorporation of freshwater
735 forcing as a result of ice sheet melt in climate models is an on-going process. Ideally,
736 the surface mass balance modelling of the ice sheets and glaciers would become part
737 of the AOGCM's to obtain consistent results and include feedbacks between the ice
738 sheets and glaciers with the rest of the climate system.

739

740 Ideally, sea-level change should be estimated on a national level, which is what
741 coastal planners are interested in, but the spatial resolution of the current sea-level
742 projections is still relatively coarse. To provide decision makers with better local
743 estimates, models will need to use finer grid resolutions to account for local effects,
744 such as coastal evolution and sediment transport. The increasing number of GPS
745 measurements is also useful for local cases, as they give better estimates of vertical
746 land motion, which can be large locally. In addition, new approaches now offer
747 possibilities to link changes in flood risk and sea-level extremes to regional SLC.

748

749 Recent regional modelling studies in the Mediterranean have pointed out the
750 relevance of the Atlantic signal, which largely contributes to the Mediterranean sea-
751 level variability and represents one of the main sources of uncertainty in sea-level
752 projections of the basin. On-going regional simulations are starting to tackle this
753 issue and show that the prescription of sea-level information from the near-Atlantic
754 at the lateral boundary significantly improves the Mediterranean sea-level
755 representation at basin-scale for hindcast periods. This will be added in future
756 scenario simulations of the Mediterranean Sea.
757

758 **Acknowledgements**

759 This paper is a result of the ISSI Workshop on Integrative Study of Sea Level, held in
760 Bern, Switzerland 2-6 February 2015.

761 A.S. is supported by a CSIRO Australia Office of the Chief Executive Fellowship and
762 the NWO-Netherlands Polar Program.

763 P.L. is funded by the European Research Council under the European Union's
764 Seventh Framework Programme (FP/2007-2013)/ERC grant agreement no. 320816.

765 Y.W. is supported by a Japan Society for the Promotion of Science (JSPS) Oversea
766 Research Fellowship (grant no. JSPS-2014-878).

767 F.A. was supported by an AXA postdoctoral fellowship.

768 **References**

- 769 Adloff, F. et al. (2015), Mediterranean Sea response to climate change in an
770 ensemble of twenty first century scenarios, *Clim. Dyn.*, doi:10.1007/s00382-
771 015-2507-3.
- 772 Agarwal, N., J. H. Jungclaus, A. Köhl, C. R. Mechoso, and D. Stammer (2015),
773 Additional contributions to CMIP5 regional sea level projections resulting from
774 Greenland and Antarctic ice mass loss, *Environ. Res. Lett.*, 10(7), 074008,
775 doi:10.1088/1748-9326/10/7/074008.
- 776 Bamber, J. L., and W. P. Aspinall (2013), An expert judgement assessment of future
777 sea level rise from the ice sheets, *Nat. Clim. Chang.*, 3(4), 424–427,
778 doi:10.1038/nclimate1778.
- 779 Bilbao, R. A. F., J. M. Gregory, and N. Bouttes (2015), Analysis of the regional pattern
780 of sea level change due to ocean dynamics and density change for 1993-2099 in
781 observations and CMIP5 AOGCM's, *Clim. Dyn.*, 45(9), 2647–2666,
782 doi:10.1007/s00382-015-2499-z.
- 783 Bordbar, M. H., T. Martin, M. Latif, and W. Park (2015), Effects of long-term
784 variability on projections of twenty-first century dynamic sea level, *Nat. Clim.*
785 *Chang.*, 5, 343–347, doi:10.1038/nclimate2569.
- 786 Bouttes, N., and J. M. Gregory (2014), Attribution of the spatial pattern of CO₂-
787 forced sea level change to ocean surface flux changes, *Environ. Res. Lett.*, 9(3),
788 034004, doi:10.1088/1748-9326/9/3/034004.
- 789 Calafat, F. M., G. Jordà, M. Marcos, and D. Gomis (2012), Comparison of
790 Mediterranean sea level variability as given by three baroclinic models, *J.*
791 *Geophys. Res.*, 117(C2), C02009, doi:10.1029/2011JC007277.
- 792 Carillo, A., G. Sannino, V. Artale, P. M. Ruti, S. Calmanti, and A. Dell'Aquila (2012),
793 Steric sea level rise over the Mediterranean Sea: present climate and scenario
794 simulations, *Clim. Dyn.*, 39(9-10), 2167–2184, doi:10.1007/s00382-012-1369-1.
- 795 Carson, M., A. Köhl, D. Stammer, A. B. A. Slangen, C. A. Katsman, R. S. W. van de Wal,
796 J. A. Church, and N. J. White (2015), Coastal Sea Level Changes , Observed and
797 Projected during the 20th and 21st Century, *Clim. Change*.
- 798 Chao, B. F., Y. H. Wu, and Y. S. Li (2008), Impact of artificial reservoir water
799 impoundment on global sea level., *Science*, 320(5873), 212–214,
800 doi:10.1126/science.1154580.
- 801 Church, J. A., N. J. White, L. F. Konikow, C. M. Domingues, J. G. Cogley, E. Rignot, J.
802 M. Gregory, M. R. van den Broeke, A. J. Monaghan, and I. Velicogna (2011),
803 Revisiting the Earth's sea-level and energy budgets from 1961 to 2008, *Geophys*
804 *Res Lett*, 38(L18601), doi:10.1029/2011GL048794.
- 805 Church, J. A. et al. (2013), Sea Level Change, in *In: Climate Change 2013: The Physical*
806 *Science Basis. Contribution of Working Group I to the Fifth Assessment Report of*
807 *the Intergovernmental Panel on Climate Change*, edited by T. F. Stocker, D. Qin,
808 G.-K. Plattner, M. Tignor, S. K. Allen, J. Boschung, A. Nauels, Y. Xia, V. Bex, and P.

809 M. Midgley, Cambridge University Press, Cambridge, United Kingdom and New
810 York, NY, USA.

811 Clark, P. U., J. A. Church, J. M. Gregory, and A. J. Payne (2015), Recent Progress in
812 Understanding and Projecting Regional and Global Mean Sea Level Change,
813 *Curr. Clim. Chang. Reports*, 1(4), 224–246, doi:10.1007/s40641-015-0024-4.

814 Cogley, J. G. (2009), A more complete version of the World Glacier Inventory, *Ann*
815 *Glaciol*, 50, 32–38.

816 CSIRO, and Bureau of Meteorology (2015), *Climate Change in Australia Information*
817 *for Australia's Natural Resource Management Regions: Technical Report*.

818 Döll, P., H. Müller Schmied, C. Schuh, F. T. Portmann, and A. Eicker (2014), Global-
819 scale assessment of groundwater depletion and related groundwater
820 abstractions: Combining hydrological modeling with information from well
821 observations and GRACE satellites, *Water Resour. Res.*, 50(7), 5698–5720,
822 doi:10.1002/2014WR015595.

823 Dyurgerov, M. B., and M. F. Meier (2005), *Glaciers and the Changing Earth System: A*
824 *2004 Snapshot*.

825 Edwards, T. L. et al. (2014), Effect of uncertainty in surface mass balance–elevation
826 feedback on projections of the future sea level contribution of the Greenland
827 ice sheet, *Cryosph.*, 8(1), 195–208, doi:10.5194/tc-8-195-2014.

828 Famiglietti, J. S. (2014), The global groundwater crisis, *Nat. Clim. Chang.*, 4(11), 945–
829 948, doi:10.1038/nclimate2425.

830 Famiglietti, J. S., M. Lo, S. L. Ho, J. Bethune, K. J. Anderson, T. H. Syed, S. C. Swenson,
831 C. R. de Linage, and M. Rodell (2011), Satellites measure recent rates of
832 groundwater depletion in California's Central Valley, *Geophys. Res. Lett.*, 38(3),
833 n/a–n/a, doi:10.1029/2010GL046442.

834 Farrell, W. E., and J. A. Clark (1976), On Postglacial Sea Level, *Geophys. J. R. Astron.*
835 *Soc.*, 46, 647–667.

836 Favier, L., G. Durand, S. L. Cornford, G. H. Gudmundsson, O. Gagliardini, F. Gillet-
837 Chaulet, T. Zwinger, A. J. Payne, and A. M. Le Brocq (2014), Retreat of Pine
838 Island Glacier controlled by marine ice-sheet instability, *Nat. Clim. Chang.*, 4(2),
839 117–121, doi:10.1038/nclimate2094.

840 Frieler, K., P. U. Clark, F. He, S. R. M. Ligtenberg, M. R. van den Broeke, R.
841 Winkelmann, R. Reese, and A. Levermann (2015), Consistent Evidence of
842 Increasing Antarctic Accumulation with Warming, *Nat. Clim. Chang.*, 5, 348–
843 352.

844 Fürst, J. J., H. Goelzer, and P. Huybrechts (2015), Ice-dynamic projections of the
845 Greenland ice sheet in response to atmospheric and oceanic warming, *Cryosph.*,
846 9(3), 1039–1062, doi:10.5194/tc-9-1039-2015.

847 Gardner, A. S. et al. (2013), A reconciled estimate of glacier contributions to sea level
848 rise: 2003 to 2009., *Science*, 340(6134), 852–7, doi:10.1126/science.1234532.

849 Giesen, R. H., and J. Oerlemans (2013), Climate-model induced differences in the
850 21st century global and regional glacier contributions to sea-level rise, *Clim.*
851 *Dyn.*, *41*(11-12), 3283–3300, doi:10.1007/s00382-013-1743-7.

852 Gleeson, T., K. M. Befus, S. Jasechko, E. Luijendijk, and M. B. Cardenas (2015), The
853 global volume and distribution of modern groundwater, *Nat. Geosci.*, *9*, 161–
854 167, doi:10.1038/ngeo2590.

855 Golledge, N. R., D. E. Kowalewski, T. R. Naish, R. H. Levy, C. J. Fogwill, and E. G. W.
856 Gasson (2015), The multi-millennial Antarctic commitment to future sea-level
857 rise, *Nature*, *526*(7573), 421–425, doi:10.1038/nature15706.

858 Gornitz, V. (1995), Sea-level rise: A review of recent past and near-future trends,
859 *Earth Surf. Process. Landforms*, *20*(1), 7–20, doi:10.1002/esp.3290200103.

860 Gregory, J. M. et al. (2013), Twentieth-century global-mean sea level rise: Is the
861 whole greater than the sum of the parts?, *J. Clim.*, *26*(13), 4476–4499,
862 doi:10.1175/JCLI-D-12-00319.1.

863 Grinsted, A., S. Jevrejeva, R. E. M. Riva, and D. Dahl-Jensen (2015), Sea level rise
864 projections for northern Europe under RCP8.5, *Clim. Res.*, *64*, 15–23,
865 doi:10.3354/cr01309.

866 Han, G., Z. Ma, H. Bao, and A. Slangen (2014), Regional differences of relative sea
867 level changes in the Northwest Atlantic: Historical trends and future
868 projections, *J. Geophys. Res. Ocean.*, *119*(1), 156–164,
869 doi:10.1002/2013JC009454.

870 Han, G., Z. Ma, N. Chen, R. Thomson, and A. Slangen (2015), Changes in Mean
871 Relative Sea Level around Canada in the Twentieth and Twenty-First Centuries,
872 *Atmosphere-Ocean*, 1–12, doi:10.1080/07055900.2015.1057100.

873 Hirabayashi, Y., Y. Zang, and S. Watanabe (2013), Projection of glacier mass changes
874 under a high-emission climate scenario using the global glacier model HYOGA2,
875 *Hydrol. Res. ...*, *7*(1), 6–11, doi:10.3178/HRL.7.6.

876 Horton, B. P., S. Rahmstorf, S. E. Engelhart, and A. C. Kemp (2014), Expert
877 assessment of sea-level rise by AD 2100 and AD 2300, *Quat. Sci. Rev.*, *84*, 1–6,
878 doi:10.1016/j.quascirev.2013.11.002.

879 Howard, T., J. Ridley, A. K. Pardaens, R. T. W. L. Hurkmans, A. J. Payne, R. H. Giesen, J.
880 A. Lowe, J. L. Bamber, T. L. Edwards, and J. Oerlemans (2014), The land-ice
881 contribution to 21st-century dynamic sea level rise, *Ocean Sci.*, *10*(3), 485–500,
882 doi:10.5194/os-10-485-2014.

883 Hu, A., and C. Deser (2013), Uncertainty in future regional sea level rise due to
884 internal climate variability, *Geophys. Res. Lett.*, *40*, 2768–2772,
885 doi:10.1002/grl.50531.

886 Huss, M., and D. Farinotti (2012), Distributed ice thickness and volume of all glaciers
887 around the globe, *J. Geophys. Res. Earth Surf.*, *117*(F4), F04010,
888 doi:10.1029/2012JF002523.

889 Huss, M., and R. Hock (2015), A new model for global glacier change and sea-level

890 rise, *Front. Earth Sci.*, 3(September), 1–22, doi:10.3389/feart.2015.00054.

891 Huss, M., G. Juvet, D. Farinotti, and A. Bauder (2010), Future high-mountain
892 hydrology: A new parameterization of glacier retreat, *Hydrol. Earth Syst. Sci.*,
893 14(5), 815–829, doi:10.5194/hessd-7-345-2010.

894 Huybrechts, P., H. Goelzer, I. Janssens, E. Driesschaert, T. Fichfet, H. Goosse, and
895 M.-F. Loutre (2011), Response of the Greenland and Antarctic Ice Sheets to
896 Multi-Millennial Greenhouse Warming in the Earth System Model of
897 Intermediate Complexity LOVECLIM, *Surv. Geophys.*, 32(4), 397–416.

898 Jevrejeva, S., A. Grinsted, and J. C. Moore (2014), Upper limit for sea level
899 projections by 2100, *Environ. Res. Lett.*, 9(10), 104008, doi:10.1088/1748-
900 9326/9/10/104008.

901 Jordà, G., and D. Gomis (2013), On the interpretation of the steric and mass
902 components of sea level variability: The case of the Mediterranean basin, *J.*
903 *Geophys. Res. Ocean.*, 118(2), 953–963, doi:10.1002/jgrc.20060.

904 Joughin, I., B. E. Smith, and B. Medley (2014), Marine Ice Sheet Collapse Potentially
905 Under Way for the Thwaites Glacier Basin, West Antarctica, *Science (80-.)*, 334,
906 735–738.

907 Konikow, L. F. (2011), Contribution of global groundwater depletion since 1900 to
908 sea-level rise, *Geophys Res Lett*, 38(L17401), doi:10.1029/2011GL048604.

909 Kopp, R. E., R. M. Horton, C. M. Little, X. Jerry, M. Oppenheimer, D. J. Rasmussen, B.
910 H. Strauss, and C. Tebaldi (2014), Probabilistic 21st and 22nd century sea-level
911 projections at a global network of tide gauge sites, *Earth's Futur.*, 383–407,
912 doi:10.1002/2014EF000239.

913 Lang, C., X. Fettweis, and M. Erpicum (2015), Future climate and surface mass
914 balance of Svalbard glaciers in an RCP8.5 climate scenario: a study with the
915 regional climate model MAR forced by MIROC5, *Cryosph.*, 9(3), 945–956,
916 doi:10.5194/tc-9-945-2015.

917 Lenaerts, J. T. M., D. Le Bars, L. van Kampenhout, M. Vizcaino, E. M. Enderlin, and M.
918 R. van den Broeke (2015), Representing Greenland ice sheet freshwater fluxes
919 in climate models, *Geophys. Res. Lett.*, 42(15), 6373–6381,
920 doi:10.1002/2015GL064738.

921 Lettenmaier, D. P., and P. C. D. Milly (2009), Land waters and sea level, *Nat. Geosci.*,
922 2(7), 452–454, doi:10.1038/ngeo567.

923 Levermann, A., P. U. Clark, B. Marzeion, G. A. Milne, D. Pollard, V. Radic, and A.
924 Robinson (2013), The multimillennial sea-level commitment of global warming,
925 *Proc. Natl. Acad. Sci. U. S. A.*, 110(34), 13745–50,
926 doi:10.1073/pnas.1219414110.

927 Levermann, A. et al. (2014), Projecting Antarctic ice discharge using response
928 functions from SeaRISE ice-sheet models, *Earth Syst. Dyn.*, 5(2), 271–293,
929 doi:10.5194/esd-5-271-2014.

930 Little, C. M., R. M. Horton, R. E. Kopp, M. Oppenheimer, G. A. Vecchi, and G. Villarini

931 (2015a), Joint projections of US East Coast sea level and storm surge, *Nat. Clim.*
932 *Chang.*, 5, 1114–1120, doi:10.1038/nclimate2801.

933 Little, C. M., R. M. Horton, R. E. Kopp, M. Oppenheimer, and S. Yip (2015b),
934 Uncertainty in Twenty-First-Century CMIP5 Sea Level Projections, *J. Clim.*, 28(2),
935 838–852, doi:10.1175/JCLI-D-14-00453.1.

936 Longuevergne, L., B. R. Scanlon, and C. R. Wilson (2010), GRACE Hydrological
937 estimates for small basins: Evaluating processing approaches on the High Plains
938 Aquifer, USA, *Water Resour. Res.*, 46(11), doi:10.1029/2009WR008564.

939 Lyu, K., X. Zhang, J. A. Church, A. B. A. Slangen, and J. Hu (2014), Time of emergence
940 for regional sea-level change, *Nat. Clim. Chang.*, 4, 1006–1010,
941 doi:10.1038/nclimate2397.

942 Marcos, M., and M. N. Tsimplis (2008), Coastal sea level trends in Southern Europe,
943 *Geophys. J. Int.*, 175, 70–82.

944 Marzeion, B., A. H. Jarosch, and M. Hofer (2012), Past and future sea-level change
945 from the surface mass balance of glaciers, *Cryosph.*, 6, 1295–1322,
946 doi:10.5194/tc-6-1295-2012.

947 McGranahan, G., D. Balk, and B. Anderson (2007), The rising tide: assessing the risks
948 of climate change and human settlements in low elevation coastal zones,
949 *Environ. Urban.*, 19(1), 17–37.

950 McInnes, K. L., J. A. Church, D. Monselesan, J. R. Hunter, J. G. O’Grady, I. D. Haigh,
951 and X. Zhang (2015), Sea-level Rise Projections for Australia: Information for
952 Impact and Adaptation Planning, *Aust. Meteorol. Oceanogr. J.*

953 Mengel, M., A. Levermann, K. Frieler, A. Robinson, B. Marzeion, and R. Winkelmann
954 (2016), Future sea level rise constrained by observations and long-term
955 commitment, *Proc. Natl. Acad. Sci.*, 201500515, doi:10.1073/pnas.1500515113.

956 Mercer, J. H. (1978), West Antarctic ice sheet and CO₂ greenhouse effect: a threat of
957 disaster, *Nature*, 271, 321–325.

958 Mitrovica, J. X., M. E. Tamisiea, J. L. Davis, and G. A. Milne (2001), Recent mass
959 balance of polar ice sheets inferred from patterns of global sea-level change,
960 *Nature*, 409, 1026–1029.

961 Moss, R. H. et al. (2010), The next generation of scenarios for climate change
962 research and assessment, *Nature*, 463(747-756), 747–756,
963 doi:10.1038/nature08823.

964 Nowicki, S. et al. (2013), Insights into spatial sensitivities of ice mass response to
965 environmental change from the SeaRISE ice sheet modeling project I:
966 Antarctica, *J. Geophys. Res. Earth Surf.*, 118(2), 1002–1024,
967 doi:10.1002/jgrf.20081.

968 Oerlemans, J., and F. M. Nick (2005), A minimal model of a tidewater glacier, *Ann.*
969 *Glaciol.*, 42, 1–6.

970 Peltier, W. R. (2004), Global Glacial Isostasy and the Surface of the Ice-Age Earth: The

- 971 ICE-5G (VM2) Model and GRACE, *Annu. Rev. Earth Planet. Sci.*, 32, 111–149.
- 972 Pokhrel, Y. N., N. Hanasaki, P. J.-F. Yeh, T. J. Yamada, S. Kanae, and T. Oki (2012),
973 Model estimates of sea-level change due to anthropogenic impacts on
974 terrestrial water storage, *Nat. Geosci.*, 5(6), 389–392, doi:10.1038/ngeo1476.
- 975 Pollard, D., and R. M. Deconto (2016), Contribution of Antarctica to past and future
976 sea-level rise, *Nature*, 531(7596), 591–597, doi:10.1038/nature17145.
- 977 Pollard, D., R. M. DeConto, and R. B. Alley (2015), Potential Antarctic Ice Sheet
978 retreat driven by hydrofracturing and ice cliff failure, *Earth Planet. Sci. Lett.*,
979 412, 112–121, doi:10.1016/j.epsl.2014.12.035.
- 980 Radić, V., and R. Hock (2011), Regionally differentiated contribution of mountain
981 glaciers and ice caps to future sea-level rise, *Nat. Geosci.*, 4,
982 doi:10.1038/NGEO1052.
- 983 Radić, V., A. Bliss, A. B. Cody, R. Hock, E. Miles, and J. G. Cogley (2014), Regional and
984 global projections of twenty-first century glacier mass changes in response to
985 climate scenarios from global climate models, *Clim. Dyn.*, 42, 37–58,
986 doi:10.1007/s00382-013-1719-7.
- 987 Rhein, M. et al. (2013), Observations: Ocean, in *In: Climate Change 2013: The*
988 *Physical Science Basis. Contribution of Working Group I to the Fifth Assessment*
989 *Report of the Intergovernmental Panel on Climate Change*, edited by T. F.
990 Stocker, D. Qin, G.-K. Plattner, M. Tignor, S. K. Allen, J. Boschung, A. Nauels, Y.
991 Xia, V. Bex, and P. M. Midgley, Cambridge University Press, Cambridge, United
992 Kingdom and New York, NY, USA.
- 993 Ridley, J., J. M. Gregory, P. Huybrechts, and J. A. Lowe (2010), Thresholds for
994 irreversible decline of the Greenland ice sheet, *Clim. Dyn.*, 35, 1049–1057,
995 doi:10.1007/s00382-009-0646-0.
- 996 Rignot, E., I. Velicogna, M. R. van den Broeke, A. Monaghan, and J. Lenaerts (2011),
997 Acceleration of the contribution of the Greenland and Antarctic ice sheets to
998 sea level rise, *Geophys Res Lett*, 38(L05503), doi:10.1029/2011GL046583.
- 999 Rignot, E., J. Mouginot, M. Morlighem, H. Seroussi, and B. Scheuchl (2014),
1000 Widespread, rapid grounding line retreat of Pine Island, Thwaites, Smith, and
1001 Kohler glaciers, West Antarctica, from 1992 to 2011, *Geophys. Res. Lett.*, 41(10),
1002 3502–3509, doi:10.1002/2014GL060140.
- 1003 Ritz, C., T. L. Edwards, G. Durand, A. J. Payne, V. Peyaud, and R. C. A. Hindmarsh
1004 (2015), Potential sea-level rise from Antarctic ice-sheet instability constrained
1005 by observations, *Nature*, doi:10.1038/nature16147.
- 1006 Robinson, A., R. Calov, and A. Ganopolski (2012), Multistability and critical thresholds
1007 of the Greenland ice sheet, *Nat. Clim. Chang.*, 2(6), 429–432,
1008 doi:10.1038/nclimate1449.
- 1009 Rodell, M., I. Velicogna, and J. S. Famiglietti (2009), Satellite-based estimates of
1010 groundwater depletion in India., *Nature*, 460(7258), 999–1002,
1011 doi:10.1038/nature08238.

- 1012 Shannon, S. R., A. J. Payne, I. D. Bartholomew, M. R. Van Den Broeke, T. L. Edwards,
1013 A. J. Sole, R. S. W. Van De Wal, and T. Zwinger (2013), Enhanced basal
1014 lubrication and the contribution of the Greenland ice sheet to future sea-level
1015 rise, , 1–6, doi:10.1073/pnas.1212647110/-
1016 /DCSupplemental.www.pnas.org/cgi/doi/10.1073/pnas.1212647110.
- 1017 Shepherd, A. et al. (2012), A Reconciled Estimate of Ice-Sheet Mass Balance, *Science*
1018 (80-), 338(6111), 1183–1189, doi:10.1126/science.1228102.
- 1019 Simpson, M. J. R., K. Breili, and H. P. Kierulf (2014), Estimates of twenty-first century
1020 sea-level changes for Norway, *Clim. Dyn.*, 42(5-6), 1405–1424,
1021 doi:10.1007/s00382-013-1900-z.
- 1022 Slangen, A. B. A., and R. S. W. van de Wal (2011), An assessment of uncertainties in
1023 using volume-area modelling for computing the twenty-first century glacier
1024 contribution to sea-level change, *Cryosph.*, 5, 673–686, doi:10.5194/tc-5-673-
1025 2011.
- 1026 Slangen, A. B. A., C. A. Katsman, R. S. W. van de Wal, L. L. A. Vermeersen, and R. E. M.
1027 Riva (2012), Towards regional projections of twenty-first century sea-level
1028 change based on IPCC SRES scenarios, *Clim. Dyn.*, 38(5-6), 1191–1209,
1029 doi:10.1007/s00382-011-1057-6.
- 1030 Slangen, A. B. A., M. Carson, C. A. Katsman, R. S. W. van de Wal, A. Koehl, L. L. A.
1031 Vermeersen, D. Stammer, and R. S. W. Van De Wal (2014), Projecting twenty-
1032 first century regional sea-level changes, *Clim. Change*, 124, 317–332,
1033 doi:10.1007/s10584-014-1080-9.
- 1034 Slangen, A. B. A., J. A. Church, X. Zhang, and D. Monselesan (2015), The sea-level
1035 response to external forcings in CMIP5 climate models, *J. Clim.*, 28(21), 8521–
1036 8539, doi:10.1175/JCLI-D-15-0376.1.
- 1037 Taylor, K. E., R. J. Stouffer, and G. A. Meehl (2012a), An overview of CMIP5 and the
1038 experiment design, *Bull Am Meteorol Soc*, 93(4), 485–498, doi:10.1175/BAMS-
1039 D-11-00094.1.
- 1040 Taylor, R. G. et al. (2012b), Ground water and climate change, *Nat. Clim. Chang.*,
1041 3(4), 322–329, doi:10.1038/nclimate1744.
- 1042 Vaughan, D. G. et al. (2013), Observations: Cryosphere, *Clim. Chang. 2013 Phys. Sci-*
1043 *ence Basis. Contrib. Work. Gr. I to Fifth Assess. Rep. Intergov. Panel Clim.*
1044 *Chang.*, 317–382, doi:10.1017/CBO9781107415324.012.
- 1045 Vizcaino, M., U. Mikolajewicz, J. Jungclaus, and G. Schurgers (2010), Climate
1046 modification by future ice sheet changes and consequences for ice sheet mass
1047 balance, *Clim. Dyn.*, 34, 301–324.
- 1048 Vries, H. de, C. Katsman, and S. Drijfhout (2014), Constructing scenarios of regional
1049 sea level change using global temperature pathways, *Environ. Res. Lett.*, 9(11),
1050 115007, doi:10.1088/1748-9326/9/11/115007.
- 1051 Wada, Y., and M. F. P. Bierkens (2014), Sustainability of global water use: past
1052 reconstruction and future projections, *Environ. Res. Lett.*, 9(10), 104003,

1053 doi:10.1088/1748-9326/9/10/104003.

1054 Wada, Y., L. P. H. van Beek, F. C. S. Weiland, B. F. Chao, Y.-H. Wu, and M. F. P.
1055 Bierkens (2012), Past and future contribution of global groundwater depletion
1056 to sea-level rise, *Geophys Res Lett*, 39(L09402), doi:doi:10.1029/2012GL051230.

1057 Wada, Y., M.-H. Lo, P. J.-F. Yeh, J. T. Reager, J. S. Famiglietti, R.-J. Wu, and Y.-H. Tseng
1058 (2016), Fate of water pumped from underground and contributions to sea-level
1059 rise, *Nat. Clim. Chang.*, doi:10.1038/NCLIMATE3001.

1060 Weertman, J. (1974), Stability of the junction of an ice sheet and an ice shelf, *J.*
1061 *Glaciol.*, 13, 3–11.

1062 Winkelmann, R., A. Levermann, M. A. Martin, and K. Frieler (2012), Increased future
1063 ice discharge from Antarctica owing to higher snowfall., *Nature*, 492(7428),
1064 239–42, doi:10.1038/nature11616.

1065 Winkelmann, R., A. Levermann, A. Ridgwell, and K. Caldeira (2015), Combustion of
1066 available fossil fuel resources sufficient to eliminate the Antarctic Ice Sheet, ,
1067 1(September), 1–5.

1068 Wisser, D., S. Froking, S. Hagen, and M. F. P. Bierkens (2013), Beyond peak reservoir
1069 storage? A global estimate of declining water storage capacity in large
1070 reservoirs, *Water Resour. Res.*, 49(9), 5732–5739, doi:10.1002/wrcr.20452.

1071 Wong, P. P., I. J. Losada, J.-P. Gattuso, J. Hinkel, A. Khattabi, K. McInnes, Y. Saito, and
1072 A. Sallenger (2013), Chapter 5: Coastal Systems and Low-Lying Areas, in *IPCC*
1073 *WGII AR5*, pp. 1–85.

1074 Yin, J. (2012), Century to multi-century sea level rise projections from CMIP5 models,
1075 *Geophys. Res. Lett.*, 39(17), doi:10.1029/2012GL052947.

1076 Yin, J., S. M. Griffies, and R. J. Stouffer (2010), Spatial Variability of Sea-Level Rise in
1077 21st Century Projections, *J. Clim.*, 23, 4585–4607, doi:10.1175/2010JCLI3533.1.

1078 Zuo, Z., and J. Oerlemans (1997), Contribution of glacier melt to sea-level rise since
1079 AD 1865: a regionally differentiated calculation, *Clim Dyn*, 13, 835–845.

1080